Journal of
Nuclear Medicine & Radiation Therapy

Nikolopoulos, et al., J Nucl Med Radiat Ther 2014, 6:1
DOI: 10.4172/2155-9619.1000201

Research Article Open Access

GATE Simulation of the Biograph 2 PET/CT Scanner

Nikolopoulos D[1*], Michail C[2], Valais I[2], Yannakopoulos P[1], Kottou S[3], Karpetas G[4] and Panayiotakis G[4]

[1]*Department of Computer Electronic Engineering, Technological Education Institute of Piraeus, Greece, Petrou Ralli & Thivon 250, 122 44, Aigaleo, Athens, Greece*

[2]*Department of Biomedical Technology Engineering, Technological Educational Institute of Athens, Agiou Spiridonos, 12210, Aigaleo, Greece*

[3]*Department of Medical Physics, Medical School, University of Athens, Mikras Asias 75, GR11527, Athens, Greece*

[4]*Department of Medical Physics, School of Medicine, University of Patras, 15310, Rion, Greece*

[*]**Corresponding author:** Nikolopoulos D, Department of Computer Electronic Engineering, Technological Education Institute of Piraeus, Greece, Petrou Ralli & Thivon 250, 122 44, Aigaleo, Athens, Greece, Tel: +0030-210-5381560; Fax: +0030-210-5381436; E-mail: dniko@teipir.gr

Received date: Oct 15, 2014, **Accepted date:** Nov 19, 2014, **Publication date:** Nov 27, 2014

Abstract

GATE is advanced open source software dedicated to numerical simulations in medical imaging and radiotherapy. It currently supports simulations of Emission Tomography (Positron Emission Tomography - PET and Single Photon Emission Computed Tomography - SPECT), Computed Tomography (CT) and Radiotherapy experiments. This work focused on the commercial Biograph 6 PET/CT scanner. The study targeted to (a) port previously developed and validated GATE codes to the currently available stable version GATE v.6.1, (b) evaluate model's validity detecting sources of bias (c) investigate differentiations imposed if different sources were employed, namely F-18 (Fluorine-18), O-15 (Oxygen-15) and C-11 (Carbon-11). The geometry of the system components was described in GATE, including detector ring, crystal blocks, PMTs etc. Energy and spatial resolution were taken into account. The GATE results were compared to experimental data obtained according to the NEMA NU-2-2001 protocol, Analysis was limited to scatter fraction, count looses and randoms. Good agreement was achieved between experimental and GATE results. Significant sources of bias were the (a) dead time value, (b) dead-time mode (paralysable-nonparalysable), (c) modelled activity (d) modelled source, (e) additional dead time values adopted in GATE modules.

Keywords: Positron emission tomography (PET); Single photon Eemission; Computed tomography - SPECT); Computed tomography (CT); Radiotherapy; GATE simulation

Introduction

Positron emission tomography (PET) is a medical diagnostic method to observe metabolism, blood flow, neurotransmission and important biochemical entities [1]. To-date, commercial PET systems employ several types of scintillators. $Be_4Ge_3O_{12}$ (BGO) has been considered, for a long time, as the state of the art [2,3]. $LuSiO_5$ (LSO) has become the best competitor due to its high detection efficiency [1,3-5]. Other scintillators, such as Gd_2SiO_5 (GSO), $LuAlO_3$ (LuAP), $YAlO_3$ (YAP) and $Y_3Al_5O_{12}$ (YAG) have been employed as well [1,3,4]. Noticeable is the recent tendency in introducing new detector types and designs [2,3,6-10]. Modern PET imaging technology involves, nowadays, algorithms for statistical effects, scatter and random coincidences, fast detector electronics and accurate reconstruction algorithms [1,3,11,12]. State-of-the art PET scanners are dual modalities, namely they incorporate computed tomography (CT) or magnetic resonance imaging (MRI) systems, to achieve more accurate anatomical localisation [12]. Especially PET/CT systems, eliminate lengthy PET transmission scans and generate complex three dimensional images within few minutes. This improves count-rate, spatial resolution and signal-to-noise ratio (SNR) [2,3,13]. Simultaneously, it enhances clinical conditions, diagnosis, follow-up and therapy [12]. PET/CT technology is undergoing rapid evolution. As the current technology becomes more widespread, it is likely that there will be a demand for PET designs of better performance and less cost [1,3]. This intensifies the interest for investigations on already employed PET systems [5,7,11,14-22] and in seeking applicability of new detector concepts. In designing and evaluating new PET systems, it is of significance to determine accurately various physical phenomena associated with radiation detection [3,4,6,7]. For example, incorrectly detected scatter and characteristic X-ray fluorescence radiation, bremsstrahlung, Auger and Koster-Kronig electrons, could result in significant degradation of spatial resolution and image contrast [18,19]. In simulating the stochastic processes involved in radiation detection, the Monte Carlo techniques constitute very efficient tools [3,4,6,7]. Several general Monte Carlo packages are available (e.g. MCNP, EGSnrcMP, GEANT4) [6,7]. All are conceptualised for complex and general geometries of particle showers; however, under non-trivial coding. From these, GATE (GEANT4 Application for Tomographic Emission) is more frequently employed in PET due to its flexibility for Tomographic simulations [16].

The present work is focused on the commercial Biograph 6 PET/CT scanner. The initiatives were diverging. At first, the study aimed to port previously developed and validated GATE codes [22] to the stable version v.6.1 of GATE. Second, it focuses on re-evaluating model's validity, however, detecting additionally some sources of bias. Additionally it is investigated the role of utilising different sources than F-18 (Fluorine-18) namely O-15 (Oxygen-15) and C-11 (Carbon-11). The geometry of the system components was described in GATE, including detector ring, crystal blocks, PMTs etc. The energy and spatial resolution of the scanner as given by the manufacturers were taken into account. The GATE results were compared to directly derived experimental data obtained according to the NEMA

NU-2-2001 protocol, Analysis was limited to scatter fraction, count looses and randoms.

Scanner and Gate Simulation

The Siemens Biograph 6 PET scanner digital geometry model has 48 detector modules, arranged in three block rings. Each one of these modules consists of three blocks in the axial direction. Each block is made of 13x13 LSO crystals 169 crystals per block. The whole scanner consists of 24,336 crystals arranged in 39 detection rings; each one has 624 crystals with 83 cm in diameter. The surface area and the thickness of the individual crystals are 4x4 mm^2 and 20 mm, respectively. In addition the scanner has an axial field of view (FOV) of 16.2 cm and transverse FOV of 58.5 cm. Figure 1 presents a characteristic GATE representation of the Biograph 6 PET scanner.

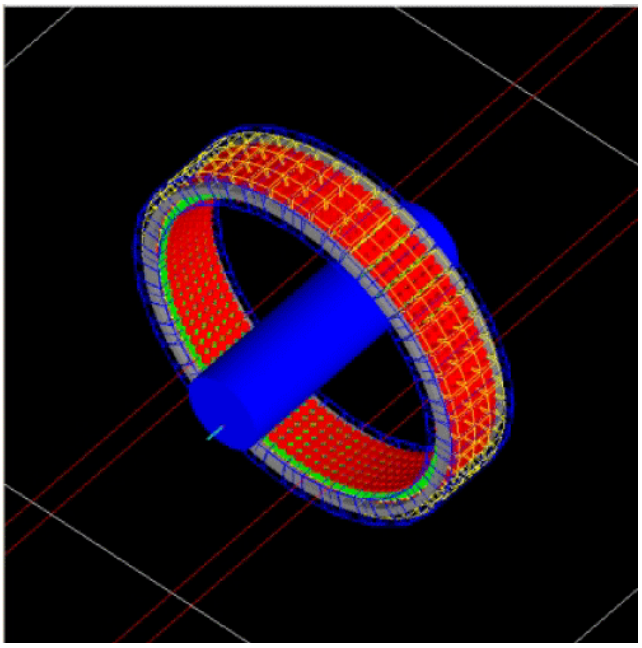

Figure 1: GATE geometry model of the Siemens Biograph Duo 6 PET scanner. Gray indicates shielding, green, LSO blocks, red PMT's, yellow light-guides and blue wire-framed parallelepipeds, PETs heads.

Previous validated GATE codes [22] developed with GATE v.3.1 under LINUX Fedora Core 3 OS, were further ported to work under the well-established version v.6.1 of GATE. GATE 6.1 was considered preferable because the developed codes presented less core malfunctions (bugs) in the certain computers that were employed in the simulations compared to the newer versions. The GATE codes simulated the following parts: (a) entire PET's detector arrangement, (b) light guides, photomultiplier tubes and related electronics, (c) coincidence circuits and processors, (d) digitizer, (e) time-delay of PET, (f) data processing systems, (g) examination bed, (h) PET's gantry, (i) lead shielding (Figure 3). Porting followed the general scheme of the previous GATE v3 codes, however, making appropriate code modifications to utilise new GATE capabilities and to improve overall approximation of modelling.

The simulation followed the philosophy of GATE, namely script-modelling of the path of particles through matter and electromagnetic fields at different levels of description, analysis and visualization. In brief, modelling of acquisition processes and detector output pulses was implemented through a chain of processing modules comprising the (i) adder which regrouped hits per volume into pulses, (ii) readout which regrouped pulses per block, (iii) energy response which modelled energy spectrum's blurring after readout, (iv) threshold electronics which provided cut-off energy windows and (vi) dead-time modules which defined the dead-time behaviour of the counting system. In detail, all particle history events (hits) were first collected from each simulated scintillator. Then a series of signal processors was inserted, referred hereafter as digitizer. Note that each signal processor of the digitizer mimics, generally, a separate portion of a real scanner's signal processing chain and that digitizer's set up is one of the most critical parts of the whole simulation [21] so as to produce results that are reasonable, realistic and comparable with previous works. In overall, the digitizer of this work processed all GATE-hits, produced all single events and simulated from these all coincidence events. Specifically, this work's digitizer involved, first, an adder module. This summed all energy deposited by particles' interactions within each simulated crystal, mimicking thus actual electronic pulses. Next, a readout module was inserted. This regrouped all simulated pulses per block into a single pulse. Then, a blurring module was employed which assigned energy resolution to the simulated LSO crystals. A mean value of 15.3% in reference to 511 keV was adopted, whereas a detection efficiency factor (0.9) was added to the Readout pulses. Next, a paralysable dead-time module was inserted to mimic actual dead-time bias on the single events level. Thereafter, at the same level, two different energy windows were employed, namely one between 200 and 650 keV and the other between 425 and 650 keV. Both were applied via thresholder and upholder modules. From these, a Singles ascii file was created, containing selected information, namely, for each single event, the energy deposited and the coordinates of detection within the modelled geometry. A coincidence sorter module was then inserted. This searched the singles list for pairs of coincident singles that could be registered within a coincidence time window of 4.5 ns. It is noted that each single carries information about all physical processes of hits and that all related coincidence analysis is based on singles, since a coincidence occurs when two singles hit two distinct detectors in the same time window. An additional paralysable delayed window was then applied of various offsets and window of 4.5 ns. Note that this method, viz. delayed coincidences, is considered adequate for the estimation of random events [22,23]. Moreover, a coincidence dead-time was further applied to the above coincidence chains. Finally, the transfer efficiency coefficient of the the LSO crystals was taken equal to 28% [3,4], the light yield equal to 27000 quanta/MeV [3,4] and the intrinsic conversion efficiency equal to 8.2% in reference to 511 keV [3,4]. In addition, this work utilised GATE's capability for full customization of modelled physical processes [21] and the ability of setting thresholds for the production of secondary electrons, X-rays and delta-rays [21]. The standard energy package was employed for the simulation of Photoelectric and Compton interactions and the Penelope model for low-energy Rayleigh scattering. Standard models were employed in the simulation of multiple scattering Following the previous GATE v3 coding, energy and range cuts were 1 cm for both photons and electrons inside LSO crystals.

Nema Count Rate Performance, Accuracy of Count Losses, Random Corrections and Validation

This work was based on the National Electrical Manufacturers Association (NEMA) performance measurements protocol NU 2-2001. This protocol is widely accepted as methodology for the assessment of individual PET system's performance [24]. It includes measurements for spatial resolution, intrinsic scatter fraction, sensitivity, count rate performance, accuracy of count losses and random corrections [24,25]. The present work employed only the parts for scatter fraction performance, accuracy of count losses and random corrections. This was because experimental measurements of the team for the Biograh 6 were conducted according to NEMA-NU-2-2001 in a previous publication [22]. Additionally, the previous GATE v3 codes were targeted to these measurements. Although the new NEMA-NU-2007 protocol [23] is now state-of-the art, the methodology for count rate performance, accuracy of count losses and random corrections remains, more or less, unchanged in respect to the corresponding NEMA-NU-2001 protocol. Accounting this fact and taking into consideration that the previous validation measurements were derived by the team according to the NEMA-NU-2001 protocol, ported methodology was decided still to follow the previous NEMA-NU-2001 standard.

The NEMA-NU-2001 scatter phantom was described in GATE v6.1. According to NEMA-NU-2001, the scatter phantom comprises a 20.3 cm diameter solid polyethylene cylinder with a 70 cm long 6.4 mm diameter hole drilled at 4.5 cm radial offset from the center of the cylinder [23]. Inside a drilled hole, a test phantom line source is inserted. The test phantom line source insert is a polyethylene coated plastic tube at of 80 cm length, with an inside diameter of 3.2 mm and an outside diameter of 4.8 mm. The central 70 cm of this tube is filled with a known quantity of activity and threaded through the 6.4 mm hole in the test phantom. The GATE model of this scatter phantom is shown in Figure 2, in blue being the main phantom, in red the drilled hole and in green the test phantom's polyethylene line source coating.

Acquisitions were modelled at different levels of activity for diverging acquisition times. Simulated activity (A) values ranged between 5 kBq and 800 MBq, the latter recommended for 3D PET in the NEMA-NU-2007 protocol [23]. Depending on simulation settings, the modelled acquisition time compensated between collecting significant number of coincidences (>106) while keeping size of the output ASCII files reasonably small.

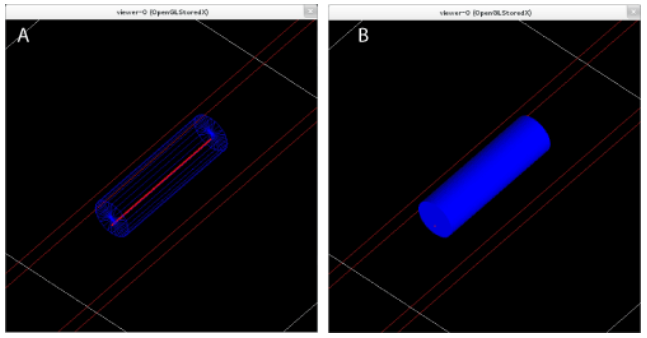

Figure 2: View of the NEMA NU2-2001 scatter fraction phantom.

Calculation Methodology

As stated in literature [21,23-25], it is important to understand the fraction of scatter and random coincidences with respect to the total count rate. This is because scatter coincidences add background noise to produced images and decrease overall contrast. Random coincidences also produce errors in count rates and, since they do not contain any spatial information, can render significant artefacts in reconstructed images [26]. On the contrary, if random and scatter coincidences are removed, a perfect radioactive point source positioned in the FOV of the camera could be reconstructed. Calculation of true, scatter and random coincidences suffers from differentiations in corresponding definitions and can be affected by user-controlled parameters in an actual PET system. In this work the following definitions were followed: (a) true coincidences were considered those having both their singles initiated from the same annihilation event. (b) scatter coincidences were considered the true coincidences for which one of the two single photons (or both) interacted with the scatter phantom, bed or GATE-world before reaching the detector. (c) random coincidences were those for which both photons, initiated from two different annihilation events and hit two different detectors in the same coincidence window.

To implement above calculations a GNU Octave program was specifically written oriented to counting prompt, true, scatter and random coincidences, according to NEMA requirements for each activity level from the corresponding GATE output files. The corresponding flowchart is given in Figure 3.

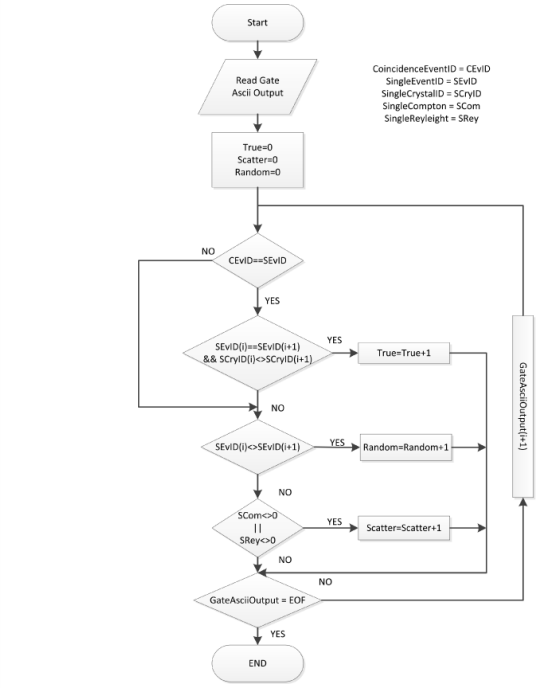

Figure 3: Flow chart for the GNU octave script that counts True, Random and Scatter coincidences.

According to Figure 3, calculations were performed from both Singles and Coincidences GATE ASCII files. The former calculation was advantageous compared to the latter one. This was because it allowed separate calculations of coincidences in bed or world prior to

detection. Note that the latter calculation cannot be performed from the output of coincidences GATE ASCII files. ASCII output was selected instead of the corresponding ROOT output. This was because it yielded to manageable outputs, smaller files that were treated very efficiently and easy under GNU octave and GNU Plot. Both latter issues were considered advantageous, since the corresponding output (a) can be also ported to Matlab and Windows OS, (b) plotting and data handling was easier than the corresponding C^{++} ROOT's driven output. It should be noted finally that the above definition of true, scatter and random coincidences is often disregarded in everyday practice. Trivial is to consider true coincidences as events that occur when both photons from an annihilation event are detected by detectors in coincidence and that neither photon undergoes any form of interaction prior to detection [27]. This distinction between true and scatter coincidences is actually adopted by the National Electrical Manufacturers Association [23,24]. To address this differentiation true and scatter coincidences, and accounting the definition adopted in this work, net true coincidences, hereafter called true coincidences, were calculated according to the following equation

$$C_{true} = C_{total} - C_{random + scatter} \quad (1)$$

which implicitly assumes that true and scatter coincidences are considered as two different types of events. Scatter Fraction (SF) was calculated as

$$SF = S/S+T \quad (2)$$

where S and T are the scattered and true coincidences respectively.

Results and Discussion

Table 1 presents one experimental and eight simulated series of count rates separated for true, random and scatter coincidences Experimental count rates were derived in a previous validated work [22], with an F-18 FDG source of 1 kBq/ml specific activity with the NEMA NU 2-2001 scatter phantom. Simulated series were calculated by the ported GATE codes adopting the complete set of parameters of the previous work [22], however by changing the deadtime value of the simulated electronics part, the simulated activity and the type of source. Six simulation series referred to an F-18 source and the remaining to a potential use of an O-15 and a C-11 source. It is noted though that the PET scanners in Greece operate only with F-18 sources. Previous validation was derived by applying 900 ns and 700 ns dead time values only on singles and by simulating low counting rates.

It may be observed from Table 1 that alterations in dead-time in electronics and activity induces noticeable changes in simulated values of true, random and scatter coincidence count-rates. Noteworthy are the simulation results given in the three last rows of Table 1. It may be seen that the changes imposed by the different simulated source (F-18, O-15, C-11) are slight when the simulated values of dead-time and activity are kept stable. Simulated scatter coincidences count rates seem to be very sensitive to changes of dead-time in electronics and activity values inserted in the GATE codes. This fact raises questions regarding results derived through GATE. To the opinion of the authors, GATE results could be accompanied by adequate sensitivity analysis on employed GATE parameters. Such analysis can assist the Medical Imaging community on the reliability and reproducibility of results reported from GATE. Nevertheless, this was not an intent of the paper and is left as future work. Despite the discrepancies, it should be emphasised that simulations of the pulse processing and coincidence generation methods of real scanners are not common in the literature [10]. A reason is that it is generally difficult to model individual components of a scanner because of limited information from manufacturers about their designs-or incomplete physical characterisation of phenomena, such as optical transport in scintillators [10,28,29]. Usually the models employ analytical dead time simulations based on experimental data from the scanner [30,31], coincidence processing algorithms [30], or fixed values for physical parameters that give reasonable agreement to experimental results [22,32]. Simulation data have also been scaled to offset sensitivity mismatches to achieve close agreement with experimental results [10,22,31,32]. The risk with these approaches is that the methods used to develop and validate the simulation models may not scale with confidence beyond the exact scanner configuration used in the validation, and may result in larger errors when used for performance prediction [1]. It is also worth to mention that according to Table 1, scatter fractions calculated through equation (2) were smaller for smaller deadtime values.

Figure 4 presents the variation of scatter fraction versus modelled activity concentrations of F-18. As modelled F-18 concentration increases, scatter fraction increases as well. It can be observed also that scatter fraction values range between 30% and 38% for concentrations up to 100 kBq/ml. Scatter fraction curve type (Figure 4) and value range, are comparable to published experimental and modelled results [33,34]. Considering low counting rates (1 kBq/ml), as specified by the NEMA NU 2-2001 protocol, the simulated scatter fractions were 31.1% both for 900 and 700 ns deadtime values, as in the previous study [22]. It is noted that at 1 kBq/ml, experimental scatter fraction was 33.4%.

Results	True coincidence rate (CPS)	Random coincidence rate (CPS)	Scatter coincidence rate (CPS)
Experimental	65%	32%	3.00%
Simulated F-18 (1) Activity:14.2MBq DT electronics:300 ns Slice-Total time:50 ms-1s	64%	34%	2.00%
Simulated F-18 (2) Activity:14.2MBq DT electronics:300 ns Slice-Total time:0 ms-1s	60%	39%	1.00%
Simulated F-18 (3) Activity:14.2MBq DT electronics: 150ns Slice-Total time:10 ms-1s	71%	28.6%	0.40%
Simulated F-18 (4) Activity:1.42MBq DT electronics: 150 ns Slice-Total time:10 ms-1s	64%	34%	2%
Simulated F-18 (5) Activity:1.42MBq DT electronics: 150 ns Slice-Total time:10 ms-1s	60%	39%	1%
Simulated F-18 (6)	66%	31%	3%

Activity:22.6MBq DT electronics: 60 ns Slice-Total time:10 ms-1s			
Simulated C-11 (7) Activity:22.6MBq DT electronics: 60 ns Slice-Total time: 50 ms-50 ms	66%	31%	3%
Simulated O-15 (8) Activity:22.6MBq DT electronics: 60ns Slice-Total time:50 ms- 50 ms	66%	30%	4%

Table 1: Comparison of experimental and simulated true, random and scatter coincidence count rates. The experimental set (first row) was derived with a F-18 source of 1 kBq/ml activity concentration. All simulations (rows 2-9) were calculated with an energy window between 425 keV and 650 keV considering no dead-time (DT) on coincidences. Each simulation result-row (rows 2-9), indicates the simulated source type (F-18, O-15, C-11), its activity, the employed DT value of simulated electronics and the running time indications, namely slice time and total running time.

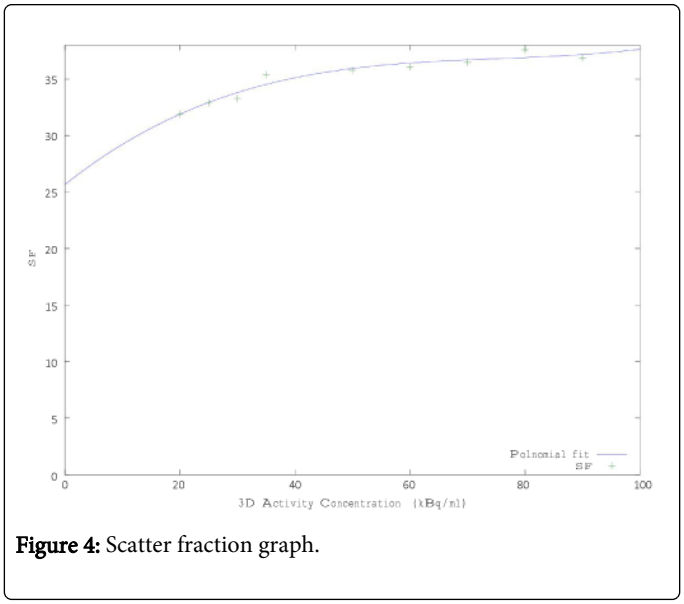

Figure 4: Scatter fraction graph.

Conclusions

In this study, previously developed and validated GATE codes were ported to the currently available stable version GATE v.6.1 and the model's accuracy was evaluated by detecting sources of bias. GATE results were compared to experimental data obtained according to the NEMA NU-2-2001 protocol, in terms of scatter fraction, count loses and random coincidences. This study showed (a) that good agreement was achieved between experimental and GATE results and (b) that potential non-negligible source of bias can be the certain values adopted for adjustable parameters of GATE such as the (i) dead time value, (ii) dead-time mode (paralysable-nonparalysable), (iii) modelled activity, (iv) modelled source, as well as the (v) additional dead time values adopted in GATE modules.

References

1. Karimian AR, Thompson C J (2008) Assessment of a new scintillation crystal (LaBr3) in PET scanners using Monte Carlo method. ?ukleonika, 53: 3-6.
2. Vandenbroucke A, Foudray AM, Olcott PD, Levin CS (2010) Performance characterization of a new high resolution PET scintillation detector.Phys Med Biol 55: 5895-5911.
3. van Eijk CW (2002) Inorganic scintillators in medical imaging.Phys Med Biol 47: R85-106.
4. van Eijk CW (2008) Radiation detector developments in medical applications: inorganic scintillators in positron emission tomography.Radiat Prot Dosimetry 129: 13-21.
5. Bailey DL, Meikle SR (1994) A convolution-subtraction scatter correction method for 3D PET.Phys Med Biol 39: 411-424.
6. Nikolopoulos D, Kandarakis I, Cavouras D, Louizi A, Nomicos C (2006) Investigation of radiation absorption and x-ray fluorescence of medical imaging scintillators by Monte Carlo Methods. Nucl. Instr. Method. (A) 565: 821-832.
7. Nikolopoulos D, Kandarakis I, Tsantilas X, Valais I, Cavouras D, et al. (2006) Comparative study of the radiation detection efficiency of LSO, LuAP, GSO and YAP scintillators for use in positron emission imaging (PET) via Monte-Carlo Methods. Nucl Instr Method (A) 569: 350-354.
8. Townsend DW (2004) Physical principles and technology of clinical PET imaging.Ann Acad Med Singapore 33: 133-145.
9. Jadvar H, Parker JA (2005) Clinical PET And PET/CT. Springer Verlag, Berlin.
10. Poon JK, Dahlbom ML, Moses WW, Balakrishnan K, Wang W, et al. (2012) Optimal whole-body PET scanner configurations for different volumes of LSO scintillator: a simulation study.Phys Med Biol 57: 4077-4094.
11. Boone JM, Seibert JA, Sabol JM, Tecotzky MA (1999) Monte Carlo study of x-ray fluorescence in x-ray detectors. Med Phys 26: 905-916.
12. Bushberg JT, Seibert JA, Leidholdt EMJ, Boone JM (1994) The essential physics of medical imaging. Lippincott Williams and Wilkins, Philadelphia.
13. Phelps ME (2004) Molecular Imaging and Its Biological Applications. Springer Verlag, Berlin.
14. Nikl M (2006) Scintillation detectors for X-rays. Meas Sci Technol 17: R37-R54.
15. Daube-Witherspoon ME, Karp JS, Casey ME, DiFilippo FP, Hines H, et al. (2002) PET performance measurements using the NEMA NU 2-2001 standard.J Nucl Med 43: 1398-1409.
16. Turco A (2012) Monte Carlo simulations of a small-animal PET scanner, Analysis of performances and comparison between camera designs. Master's Thesis at KTH-STH, TRITA: 32.
17. Bolus NE, George R, Washington J, Newcomer BR (2009) PET/MRI: the blended-modality choice of the future?J Nucl Med Technol 37: 63-71.
18. Karakatsanis N, Sakellios N, Tsantilas NX, Dikaios N, Tsoumpas C, et al. (2006) Comparative evaluation of two commercial PET scanners, ECAT EXACT HR+ and Biograph 2, using GATE. Nucl Instr Meth (A) 571: 368-372.
19. Zeraatkar N, Ay MR, Kamali-Asl AR, Zaidi H (2011) Accurate Monte Carlo modeling and performance assessment of the X-PET subsystem of the FLEX triumph preclinical PET/CT scanner.Med Phys 38: 1217-1225.
20. Mineev O, Kudenko Y, Musienko Y, Polyansky I, Yershov N (2011) Scintillator detectors with long WLS fibers and mulit-pixel photodiodes. JINST 6: 1-9.
21. Geramifar P, Ay MR, Shamsaie Zafarghandi M, Sarkar S, Loudos G, et al. (2011) Investigation of time-of-?ight bene?ts in an LYSO-based PET/CT scanner:A Monte Carlo study using GATE. Nucl. Instrum. Meth. (A) 641: 121-127.

22. Gonias P, Bertsekas N, Karakatsanis NA, Saatsakis G, Nikolopoulos D, et al. (2007) Validation of a GATE model for the simulation of the Siemens PET/CT Biograph 6 scanner. Nucl Instrum Meth (A) 571: 263-266.
23. National Electrical Manufacturers Association (2007) NEMA Standards Publication: Performance Measurements of Positron Emission Tomographs: 13-21.
24. http://depts.washington.edu/nucmed/IRL/pet_intro
25. Shimizu S, Pepin CM,.Lecomte R (2010) Assessment of Lu1:8Gd0:2SiO5 (LGSO) Scintillators with APD Readout for PET/SPECT/CT Detectors. IEEE T Nucl Sci 57: 1512-1517.
26. Lewellen TK (2008) Recent developments in PET detector technology.Phys Med Biol 53: R287-317.
27. Nakamori T, Kato T, Kataoka J, Miura T, Matsuda H, et al. (2012) Development of a gamma-ray imager using a large area monolithic 4×4 MPPC array for a future PET scanner. JINST 7: 1-13.
28. Bonifacio DAB, Belcari N, Moehrs S, Moralles M, Rosso V, et al. (2010) A Time Ef?cient Optical Model for GATE Simulation of a LYSO Scintillation Matrix Used in PET Applications. IEEE Trans Nucl Sci 57: 2483-2489.
29. van der Laan DJ, Schaart DR, Maas MC, Beekman FJ, Bruyndonckx P, et al. (2010) Optical simulation of monolithic scintillator detectors using GATE/GEANT4.Phys Med Biol 55: 1659-1675.
30. Schmidtlein CR, Kirov AS, Nehmeh SA, Erdi YE, Humm JL, et al. (2006) Validation of GATE Monte Carlo simulations of the GE Advance/ Discovery LS PET scanners.Med Phys 33: 198-208.
31. Michel C, Eriksson L, Rothfuss H, Bendriem B (2006) In?uence of crystal material on the performance of the HiRez 3D PET scanner: a Monte Carlo study. IEEE Nuclear Science Symp Conf: 2528–2531.
32. Jan S, Comtat C, Strul D, Santin G, Trbossen R (2005) Monte Carlo simulation for the ECAT EXACT HR+ system using GATE. IEEE Trans Nucl Sci, 52: 627-633.
33. Karpetas GE, Michail CM, Fountos GP, Valsamaki PN, Kandarakis IS, et al. (2013) Towards the optimization of nuclear medicine procedures for better spatial resolution, sensitivity, scan image quality and quantitation measurements by using a new Monte Carlo model featuring PET imaging. Hell J Nucl Med 16: 111-120.
34. Mawlawi O, Podoloff DA, Kohlmyer S, Williams JJ, Stearns CW, et al. (2004) Performance characteristics of a newly developed PET/CT scanner using NEMA standards in 2D and 3D modes.J Nucl Med 45: 1734-1742.